

Synthesis of ultramarine pigments from Na-A zeolite derived from kaolin waste from the Amazon

R. A. MENEZES^{1,*}, S. P. A. PAZ^{1,2}, R. S. ANGÉLICA¹, R. F. NEVES¹,
R. NEUMANN³, F. R. L. FAULSTICH³ AND S. B. C. PERGHER⁴

¹ Instituto de Geociências, Laboratório de Caracterização Mineral, UFPA – Universidade Federal do Pará, Belém, PA 66075-110, Brazil

² Faculdade de Engenharia de Materiais, UFPA – Universidade Federal do Pará, Campus Ananindeua, Belém, Brazil

³ CETEM – Centro de Tecnologia Mineral, Rio de Janeiro, RJ, Brazil

⁴ Instituto de Química, UFRN – Universidade Federal do Rio Grande do Norte, Natal, RN, Brazil

(Received 18 August 2016; revised 15 December 2016; Editor: George Christidis)

ABSTRACT: Ultramarine pigments were synthesized successfully from Na-A zeolite derived from kaolin waste. Na-A zeolite encapsulates the sulfur species formed and which act as chromophores, which circumvents their oxidation and the subsequent liberation of high levels of toxic gases during the reaction. Different Na-A zeolite matrices with various grain sizes (fine to coarse) were mixed with sulfur and sodium carbonate in various proportions to study the influence of these variables on the pigments' colours and hues. After calcination at 500°C for 5 h, the products were characterized by X-ray diffraction, X-ray fluorescence and Raman spectroscopy and were classified by the Munsell system (colour and hue). Products with colour ranging from blue to green with various hues were obtained. Both colour and hue were affected by the amount of additives and by the particle size.

KEYWORDS: kaolin waste, Na-A zeolite, ultramarine pigments.

Since the 1970s mining has been one of the main activities driving the economy of the state of Pará in northern Brazil. The mineral extraction, processing and transformation industries supply the national and world markets with various commodities including secondary kaolin, which is used for fillers and coatings in the paper industry and is one of the most widely used materials in this sector. The three biggest secondary kaolin processors in Brazil are located in the state of Pará (Imerys Rio Capim Caulim SA; Imerys, Caulim da Amazônia SA – CADAM; and Pará Pigmentos S/A – PPSA). Together, these companies supply 80%

of the total exports of this mineral from Brazil. Although this figure represents just 5% of total world kaolin production, Brazil is the only country that provides the mineral post-processing, *i.e.* ready to be used by the paper industry (Brasil, 2016).

The paper industry demands kaolin which has an extremely fine particle size ($\varnothing < 2 \mu\text{m}$) and which is extremely white; these requirements can only be met by creating a huge amount of waste, ~1 million tons per year in Brazil alone. This waste originates from the stages of granulometric separation and whitening and is disposed of in sedimentation lakes that occupy extensive areas (Carneiro *et al.*, 2003; Barata *et al.*, 2005; Maia *et al.*, 2007, 2008; Paz *et al.*, 2010). No sustainable, alternative use for the waste clay has yet been developed.

*E-mail: raquel_arn@hotmail.com
<https://doi.org/10.1180/claymin.2017.052.1.06>

The waste consists predominantly of kaolinite, with very small amounts of impurities (quartz and Fe-, Ti-bearing minerals), and constitutes an excellent source of Si and Al which could be used in the production of microporous aluminosilicates, LTA-type (Linde type A) zeolites and sodalite. Currently the waste is discarded because its particle size is not adequate for paper-production purposes (Maia *et al.*, 2007, 2008; Paz *et al.*, 2010).

The production of A-type zeolite from kaolin is a well known process. It can be prepared both from raw (*in natura*) kaolin and from thermally treated kaolin (metakaolin) (Alkan *et al.*, 2005; Heller-Kallai & Lapidés, 2007; Lapidés & Heller-Kallai, 2007; Rigo *et al.*, 2009). The exchangeable cations may be Na⁺, K⁺ or Ca²⁺, the last two being introduced by cation exchange. The cation will determine the size of the pore opening, which can have diameters of 3, 4 or 5 Å for K⁺, Na⁺ and Ca²⁺, respectively. Such flexibility is useful for various applications, including the production of ultramarine pigments (Kowalak *et al.*, 1999; Jankowska & Kowalak, 2008; Bieseki *et al.*, 2013; Menezes *et al.*, 2014).

The history of ultramarine pigments began in ancient times, when an intensely blue rock type, lapis lazuli, was used in jewellery and decorative works. The main mineral present in lapis lazuli is lazurite, a tectosilicate which can also be considered as a zeolite structure. Lazurite was considered to be of great importance in the Middle Ages; it was applied, as a powder, in the preparation of valuable pigments used in ornaments, pharaonic pieces and cathedral coatings (Loera *et al.*, 2006). Large extraction and logistical costs prompted the search for synthetic pigments which were similar to lazurite (Tarling *et al.*, 1988). In 1820, Jean-Baptiste Guimet calcined a mixture of kaolin, sulfur and sodium carbonate and obtained a blue pigment that was named 'ultramarine' (Kowalak *et al.*, 1995). Although it was economically viable, this process was considered to be inappropriate after it was revealed to be environmentally damaging due to the liberation of gases with high levels of sulfur. The changes in this process that were necessary to reduce the harmful sulfur volatiles made production too expensive (Kowalak *et al.*, 2004), and a new search began for alternative routes of synthesis of ultramarine pigments.

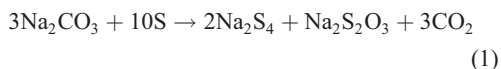
A process using a zeolitic matrix appears to offer some promise as an alternative to the Guimet process which uses kaolin. Indeed, besides decreasing the energy costs (lower temperatures are used) and the amount of additives (it uses less sulfur), the emission of sulfur oxides during the calcination is reduced

(Kowalak *et al.*, 1999). Unlike the process with kaolin, the zeolite process avoids the formation of damaging gases by hampering the hydrolysis and/or oxidation reactions through the encapsulation of the sulfur compounds within the sodalite cage or within the pores (Gobeltz *et al.*, 2011). In fact, new processes have been developed to obtain such pigments (*e.g.* Lewicka, 2016), which used quartz-feldspar as the starting material.

Two main methods have been described for the synthesis of ultramarine pigments from A-type zeolite (Gobeltz *et al.*, 2011): (1) an *ex situ* process where the zeolite is first impregnated with a solution of sodium polysulfide before calcination; and (2) an *in situ* process where sulfur and sodium carbonate are mixed into the zeolite and the polysulfides are formed during the calcination.

The formation of different sulfur species in various proportions results in diverse colours and hues. The species usually responsible for the blue colour in ultramarine zeolitic pigments is known to be the chromophore S₃⁻, whereas the chromophore S₂⁻ confers a yellow colour. Thus, mixtures of these two chromophores in various proportions lead to blue and green pigments of different hues (Booth *et al.*, 2003). The species S₆²⁻ can also act as a yellow chromophore (Gobeltz *et al.*, 2011).

Sodium polysulfides, which are generally used in the synthesis of ultramarine pigments, are usually obtained from the reaction between sulfur and sodium carbonate. The molar proportion of these two reactants (S/Na₂CO₃) affects the formation of chromophores which, in turn, determines the colour and hue of the pigment (Loera *et al.*, 2006). Among the possible reactions forming sodium polysulfides, sodium tetrasulfide (Na₂S₄) and sodium thiosulfate (Na₂S₂O₃) are favoured during calcination at <550°C (equation 1) (Gobeltz *et al.*, 1998a). The presence of any remaining sulfur after the formation of Na₂S₄ yields other sodium polysulfides, even during cooling. This behaviour is due to the metastability of polysulfides at any temperature and is attributed to the pronounced thermochromic effect presented. These effects lead to the formation of sodium polysulfides from Na₂S₃ to Na₂S₄ and consequently change the colour of pigments due to radical dimerization.



In addition to the proportion of sulfur and sodium carbonate, other factors may also affect the formation

TABLE 1. Identification of products.

Sulfur/Na ₂ CO ₃ ratio	ZA-K	ZA-KW
R1 1:1	P1-K	P1-KW
R2 1:2	P2-K	P2-KW
R3 2:1	P3-K	P3-KW

of chromophoric species such as the chemical composition of the starting zeolite, calcination temperature and oxidant atmosphere (Gobeltz *et al.*, 1998b). According to previous studies (Kowalak *et al.*, 2005), the size of the exchangeable cation affects the colour and hue because large cations favour the formation of S₂⁻ whereas smaller cations favour the formation of S₃⁻. Furthermore, the different cation sizes modify the visible light absorption frequency by the chromophores, which can also cause differences in colour and hue of the pigment.

In this context, the present work aimed to prepare ultramarine pigments from Na-A zeolite derived from kaolin waste from the Amazon using a low-cost and sustainable production. In other words, the intention was

to convert a mineral waste to a raw material for zeolite production with the main advantage being a cheaper alternative than the traditional hydrogel processes or even the processed kaolin. In addition, a comparison was carried out between pigments obtained from zeolites that used processed kaolin and kaolin waste.

EXPERIMENTAL

Starting materials

Two kaolin samples were used as sources of Si and Al in the synthesis of Na-A zeolite: processed kaolin (K) and kaolin waste (KW). Both were supplied by Imerys Rio Capim Caulim SA, which is located in the industrial district of Barcarena, State of Pará, Brazil.

Synthesis of Na-A zeolite

Na-A zeolites derived from processed kaolin (ZA-K) and from kaolin waste (ZA-KW) were obtained by hydrothermal synthesis, under reflux (Maia *et al.*, 2007; Paz *et al.*, 2010), as follows: 200 g of K and KW calcined at 700°C were mixed with 600 mL of 5 mol/L

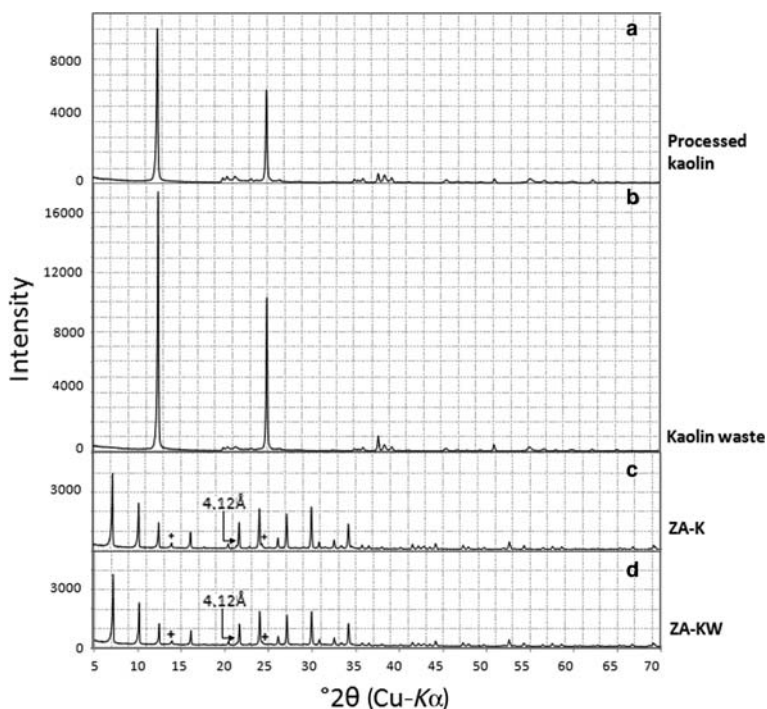


FIG. 1. XRD patterns of: (a) processed kaolin; (b) kaolin waste; (c) ZA-K; and (d) ZA-KW. + indicates sodalite.

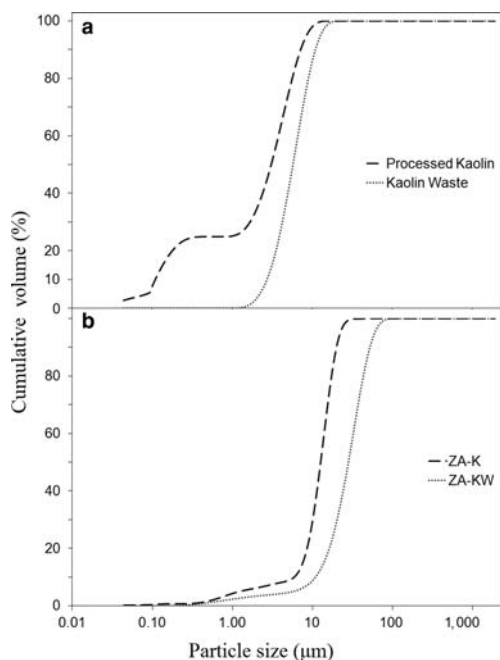


FIG. 2. Particle-size distributions of the: (a) processed kaolin and kaolin waste; and (b) zeolitic products ZA-K and ZA-KW.

NaOH solution (Vetec) at 95°C in a 1 L glass reactor under mechanical stirring for 2 h. After reaction, the samples were rinsed with distilled water until pH \approx 7 and were dried at 105°C for 24 h.

Synthesis of zeolitic pigments

Mixtures of 1 g of each Na-A zeolite and 0.5 g of sulfur + Na₂CO₃ at the relative proportions listed in Table 1 were prepared and homogenized without

reducing agent. The reactants were supplied by Synth and Nuclear, respectively. The mixtures were ground and calcined at 500°C for 5 h, under atmospheric pressure, in closed porcelain crucibles, in accord with previous work (Kowalak & Jankowska, 2003). After calcination, the products were rinsed with distilled water until pH \approx 7, and dried subsequently at 105°C for 24 h. Table 1 summarizes the pigments produced.

To facilitate comparison, the same amount of Na-A zeolite used in the synthesis of pigments was calcined without sulfur and sodium carbonate (ZA-K-CAL and ZA-KW-CAL).

Characterization of materials

The kaolin samples (processed and waste), the Na-A zeolites derived before and after calcination, and the zeolitic pigments produced were characterized by the following techniques:

Chemical analysis. The chemical composition of the materials used was determined by X-ray fluorescence spectroscopy (XRF) using an Axios-Minerals WD sequential spectrometer (PANalytical), with ceramic X-ray tube and a rhodium anode of maximum 2.4 kW power level. The specimens were prepared as glass disks (1 g of sample plus 8 g of lithium metaborate), using the IQ+ program of PANalytical's SuperQ Manager. Loss on ignition (LOI) was determined on independent test portions by heating for 1 h at 1000°C in a muffle furnace.







X-ray diffraction (XRD). The powder X-ray diffractometer employed was a Panalytical X'Pert PRO MPD with a ceramic X-ray tube (λ Cu-K α 1 = 0.1540598 nm), K β Ni filter and an X'celerator PSD (position-sensitive detector). The following analytical conditions were

TABLE 2. Chemical composition of the kaolin and zeolite samples.

Components (%)	Processed kaolin	Kaolin waste	ZA-K	ZA-KW
SiO ₂	45.21	46.13	34.63	33.30
Al ₂ O ₃	39.14	38.97	29.57	27.65
Fe ₂ O ₃	0.64	0.57	0.34	0.39
TiO ₂	0.41	0.3	0.21	0.18
Na ₂ O	0.32	–	17.52	20.02
K ₂ O	<0.1	<0.1	0.01	0.02
P ₂ O ₅	0.11	<0.1	0.03	–
LOI	14.14	13.99	17.65	18.43

LOI, Loss on ignition; –, below the detection limit.

TABLE 3. Classification of pigments according to the Munsell colour system.

Sample	P1-K	P2-K	P3-K	P1-KW	P2-KW	P3-KW
Colour	Light green	Olive green	Light green	Dark green	Light green	Blue
Munsell Classification	7.5GY 4/6	5Y 6/3	10GY 5/6	10G 3/4	10GY 5/4	7.5BG 4/8
Zeolitic Pigment						

used: scan range of $5-76^{\circ}2\theta$, probe voltage and current of 40 kV and 30 mA, respectively, $0.02^{\circ}2\theta$ step size and 60 s time/step; divergent slit of $1/8^{\circ}$ and anti scattering of $1/4^{\circ}$; mask of 10 mm; sample movement was set to spinning with a rotation time of 1.0 s.

Particle size distribution (PSD). The equipment used was an Analysette 22 Micro Tec Plus (Fritsch) using the spherical particle model, the kaolinite refractive index

($n = 1.55$) and water as a dispersing agent ($n = 1.333$). One hundred scans were carried out ($2''$ shots per scan ($n = 4$), maximum time = 7 s) in the range $0.08-2000 \mu\text{m}$ and beam obscuration between 13 and 18%.

Raman spectroscopy and photomicrographs. The Raman spectra were recorded in the range 4000 to 100 cm^{-1} using a confocal microspectrometer LabRAM HR 800 (Horiba Jobin-Yvon) with a thermo-electrically

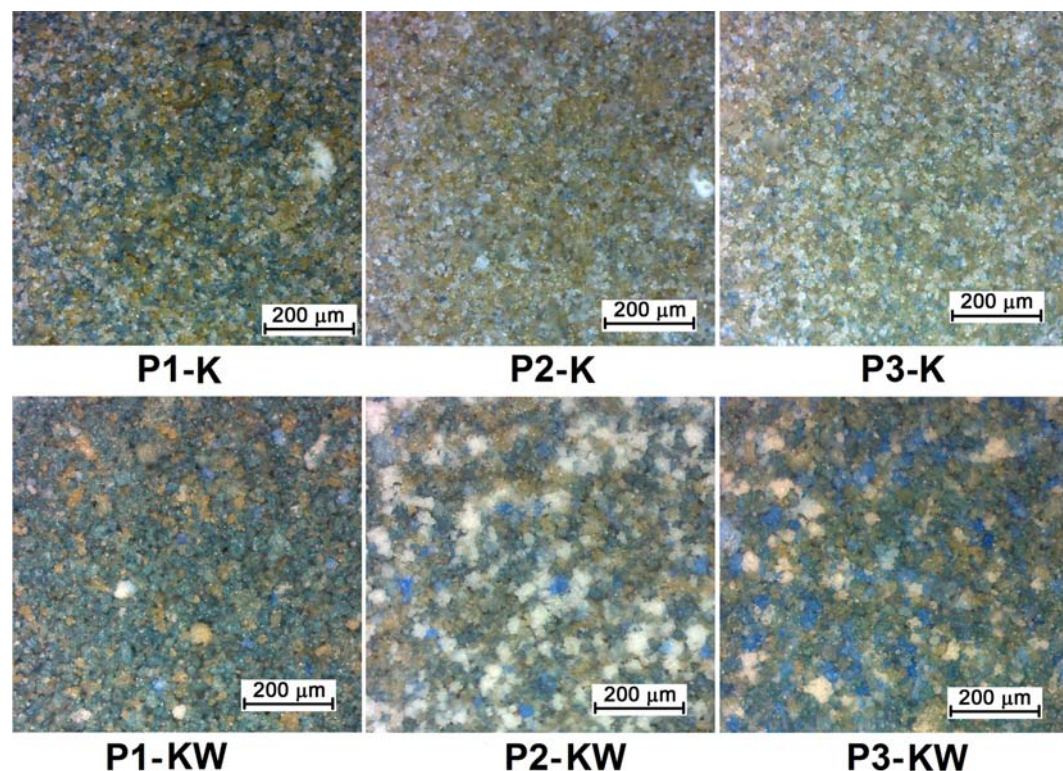


FIG. 3. Photomicrographs of synthetic grains of zeolitic pigments.

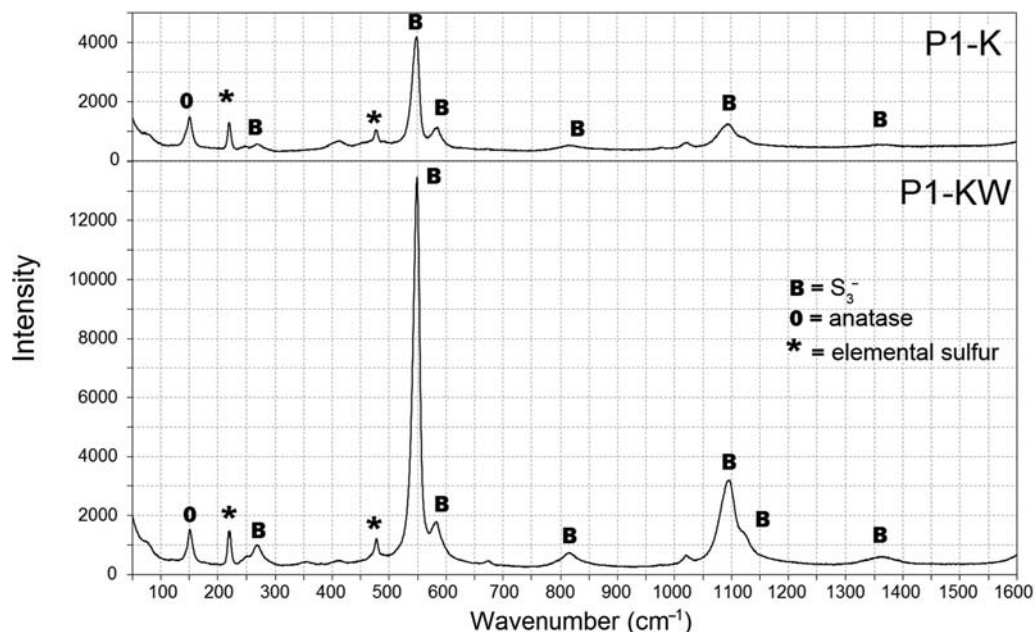


FIG. 4. Raman spectra of the blue grains of pigments P1-K and P1-KW.

cooled CCD detector. The photomicrographs were obtained using an Olympus Optical microscope.

The Munsell colour system used to determine the colour and hue of the pigments synthesized classifies the colours in a tridimensional way in the H/V/C system, where H is the hue, V is the value (lightness) and C is the chroma. The letters B, Y and G indicate the hues between the colours blue, yellow and green, respectively.

RESULTS

Processed kaolin, kaolin waste and zeolitic products derived

The diffraction patterns of the kaolin samples, of the processed kaolin (K) and of the kaolin waste (KW) are shown in Fig. 1a,b. Kaolinite is the only phase detected in both samples, which demonstrates that the materials are monomineralic and that any mineral impurities are present in amounts which are below the detection limit. The particle-size distributions of K and KW are clearly different from each other (Fig. 2a). As expected, the processed kaolin (final product for paper coatings) has a much finer particle size than the coarse kaolin waste.

Figure 1c,d shows the XRD patterns of zeolitic products. In both cases, Na-A zeolite is the dominant phase and $d_{531} = 4.12 \text{ \AA}$ ($21.34^\circ 2\theta$) determines the

sodium type (zeolite 4A). The symbol '+' indicates the formation of a small amount of sodalite (Ding *et al.*, 2010). Figure 2b shows the particle-size distribution of the zeolitic products, which are clearly different. The product derived from K has a much finer particle size than the product derived from KW.

The results of the chemical analysis (Table 2) show that SiO_2 and Al_2O_3 are the main components of both the K and KW samples, and the ratio $\text{Si}/\text{Al} \approx 1$, is typical of kaolinite. The relatively small TiO_2 levels may be related to the anatase commonly found in the kaolins of the Amazon region (Carneiro *et al.*, 2003; Barata *et al.*, 2005; Barata & Angélica, 2012). Anatase was not detected, however, because the amount was below the detection limit of XRD. Table 2 also shows that the production of Na-A zeolites incorporates substantial amounts of sodium. The levels of impurities are <1%.

Zeolitic pigments

Taking the visual observations and Munsell classification (Table 3) into consideration, only one pigment of the six produced had a blue colour; the remaining pigments were green of various hues. The particle size of the zeolitic material, which is related to the starting K sample, had the greatest impact in terms of determining the colour and hue of the pigments synthesized, *i.e.* was more influential than the sulfur/ Na_2CO_3 ratio.

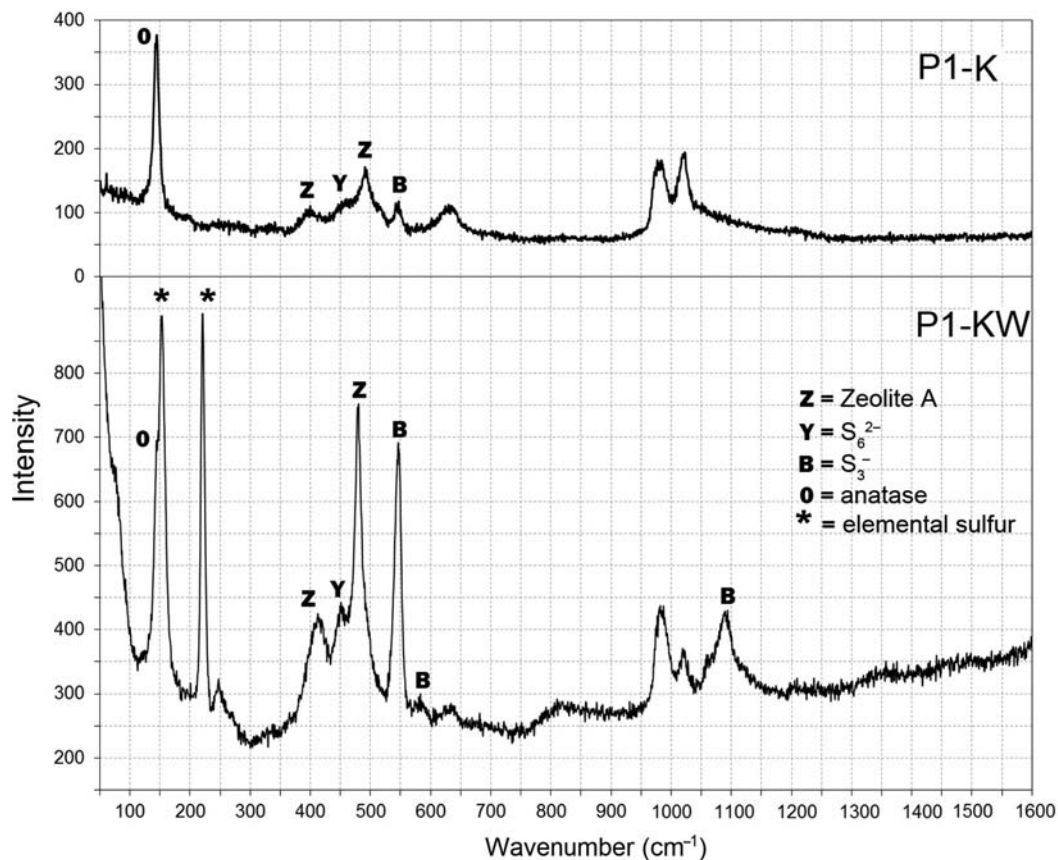


Fig. 5. Raman spectra of white grains of pigments P1-K and P1-KW.

The starting material with a finer particle size (ZA-K) produced green pigments with lighter hues (P1-K and P2-K) than those produced with materials of coarser particle size (ZA-KW producing P1-KW and P2-KW) when using the same sulfur/ Na_2CO_3 ratios for the same amount of zeolite. The ultramarine blue pigment could only be obtained using the R3 ratio (sulfur $>$ Na_2CO_3) and with a coarser starting material, which shows the strong influence of the particle size on the pigment colour. It is clear that molecular diffusion might be influenced by the average particle size and consequently interferes in species formation. Due to crystal size, larger molecules would need more time to diffuse to the interior of the sodalite cage. Considering the same reaction conditions, a small particle size favours the formation of yellow species while a larger size favours the blue colour.

Both particle size and the sulfur/ Na_2CO_3 ratio affect the type and amount of chromophores, S_3^- , S_2^- and/or S_6^{2-} , which are extremely relevant factors in

determining the colour and hue of the pigment (Booth *et al.*, 2003). Thus, the types, amounts and interactions of chromophores with the zeolite structures may be discussed based on the optical microscopy, Raman spectroscopy, XRD and XRF results (see below).

The mixture of at least four main colours (white, yellow, blue and green) can be observed in the photomicrographs shown in Fig. 3. The colours are related to the following factors: (1) white – to the unreacted starting material; (2) yellow – to the presence of unreacted elemental sulfur or the formation of chromophores S_2^- and S_6^{2-} ; (3) blue – to the presence of the S_3^- chromophore; and (4) green – to the mixture of the blue and yellow chromophores. Each of the colours observed under the optical microscope was then analysed using Raman microanalysis. In the present study only the spectra of pigments P1-K and P1-KW are shown because there were many spectral similarities among pigments derived from the same

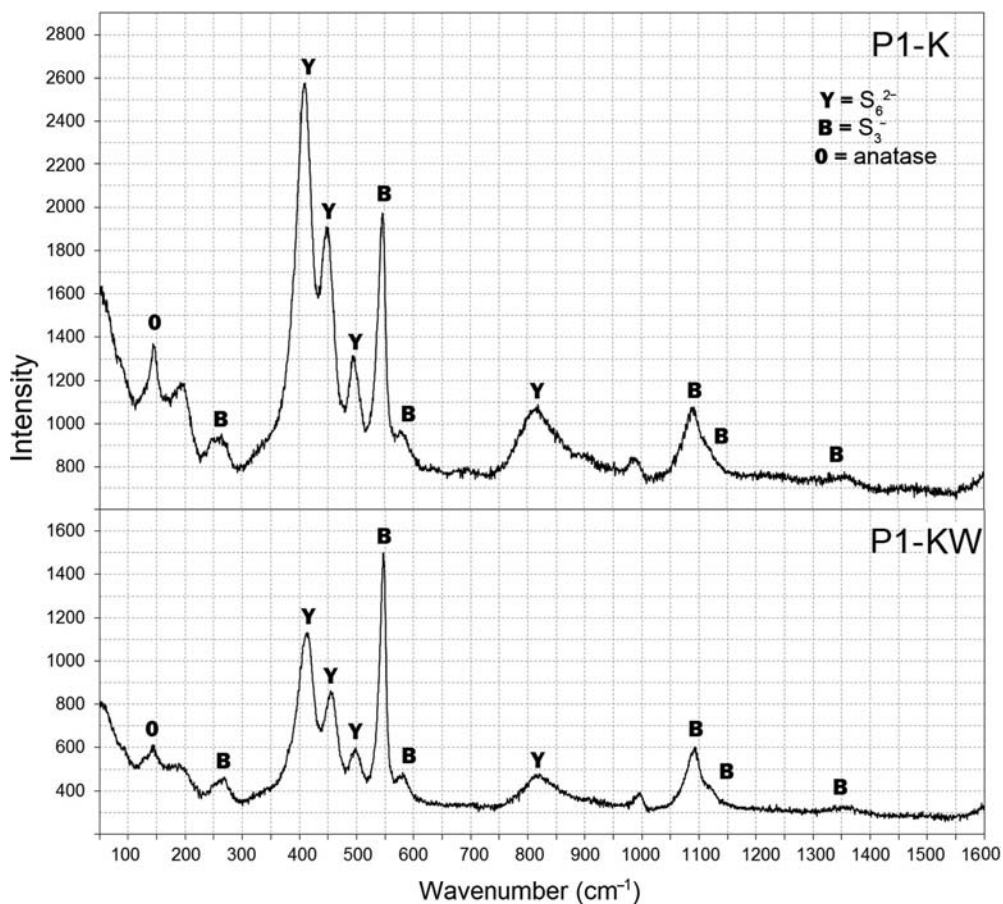


Fig. 6. Raman spectra of yellow grains of pigments P1-K and P1-KW.

zeolitic matrix. Our conclusions for these pigments can be extended to the remaining pigments, therefore.

In the blue grains (Fig. 4), the main stretching modes observed at 550 cm^{-1} (ν_1) and 260 cm^{-1} (ν_2), were assigned to S_3^- ; the same holds for the 590 cm^{-1} band, which corresponds to antisymmetric stretching (ν_3) (Ledé *et al.*, 2007; Gobeltz *et al.*, 2011). The intensity of the 550 cm^{-1} band in the P1-KW pigment is almost three times greater than in P1-K, which implies that the green hue of P1-KW is darker than that in P1-K. The same is observed for the pairs P2-KW/P2-K and P3-KW/P3-K; although the P3-KW blue pigment had already indicated a larger amount of the chromophore S_3^- as a function of the larger number of blue grains in the photomicrograph (Fig. 3). Thus, the best conditions in which to obtain the chromophore S_3^- , and therefore, the ultramarine blue pigment, was to use the R3 ratio (sulfur > Na_2CO_3) and the coarser zeolite particle size.

The spectra for the white spots indicate the presence of Na-A zeolite with bands at 392 , 490 and 635 cm^{-1} (Fig. 5). These are frequently masked due to fluorescence and are thus of relatively lower intensity, especially for finer materials (Gerrits *et al.*, 1997). The band at 144 cm^{-1} is assigned to anatase, which, being an excellent scatterer, shows high intensities even at low concentrations (Murad & Köster, 1999). In addition, bands assigned to elemental sulfur and to chromophores S_6^{2-} and S_3^- are also present.

The yellow colour in zeolitic pigments is attributed to three main agents: S_2^- (Kowalak & Jankowska, 2003), elemental sulfur (Loera *et al.*, 2006), and S_6^{2-} (Gobeltz *et al.*, 2011). The spectra of yellow grains (Fig. 6) show that the band at $\sim 580\text{ cm}^{-1}$, which is usually assigned to the stretching mode ν of S_2^- , is not confirmed by the band at 1160 cm^{-1} (2ν). Neither were the major characteristic bands of elemental sulfur

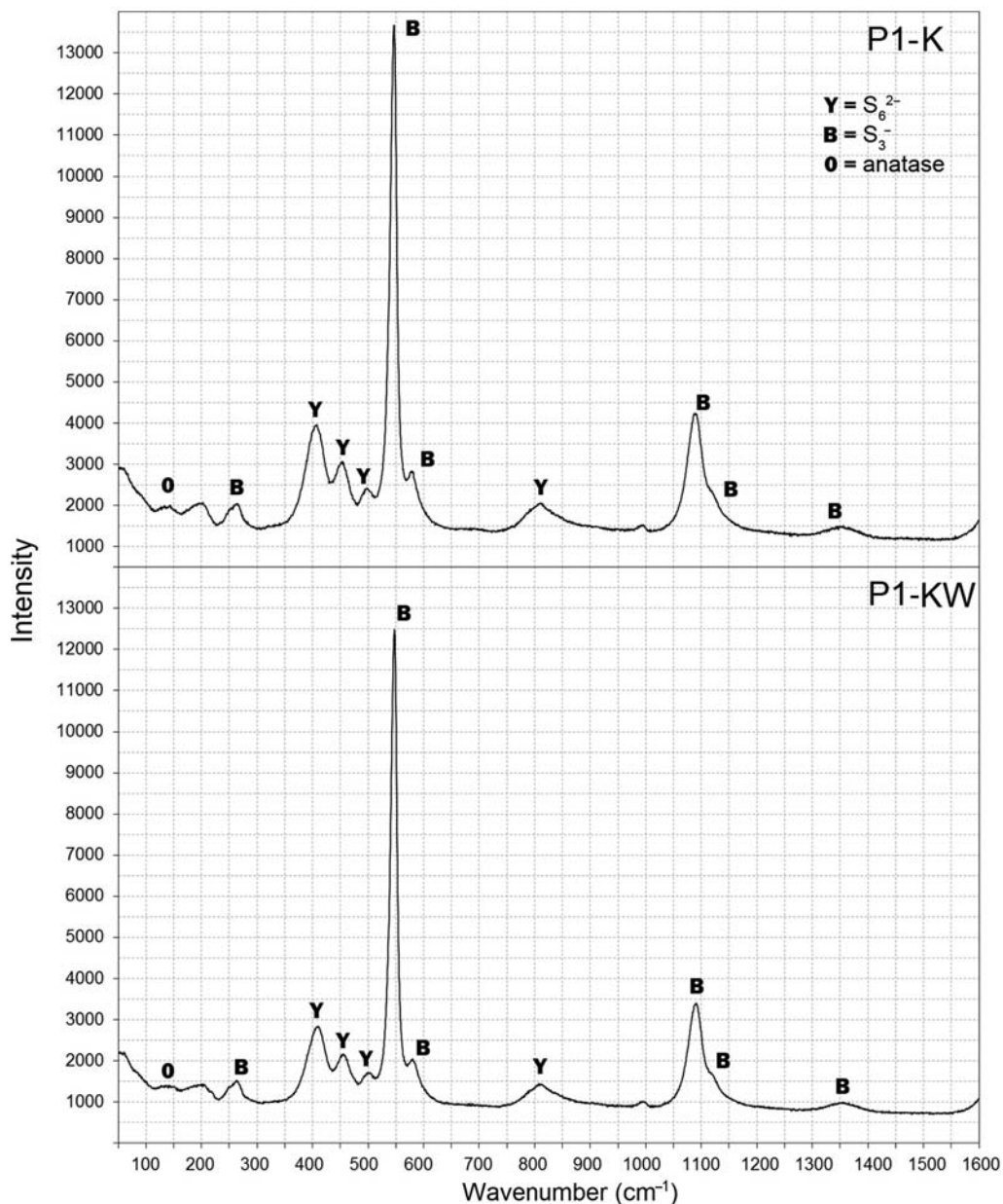


Fig. 7. Raman spectra of green grains of pigments P1-K and P1-KW.

detected at 153, 219 or 473 cm^{-1} . Finally, the overlapped band of the first three stretching harmonics at 406, 446 and 493 cm^{-1} occurs at 810 cm^{-1} , which indicates the presence of S_6^{2-} , suggesting that this species is responsible for the yellow colour.

In the green grains, the chromophore S_3^- always appears with a greater intensity than S_6^{2-} for all

pigments (Fig. 7). However, the intensity ratios between the bands at 550 and 473 cm^{-1} for the zeolitic pigments derived from K were always smaller than those for the samples derived from KW. The smaller S_3^- levels in the K samples justify the lighter hues observed. Thus, the species S_6^{2-} was shown to be more stable than the species S_3^- in the pigments derived from ZA-K due to

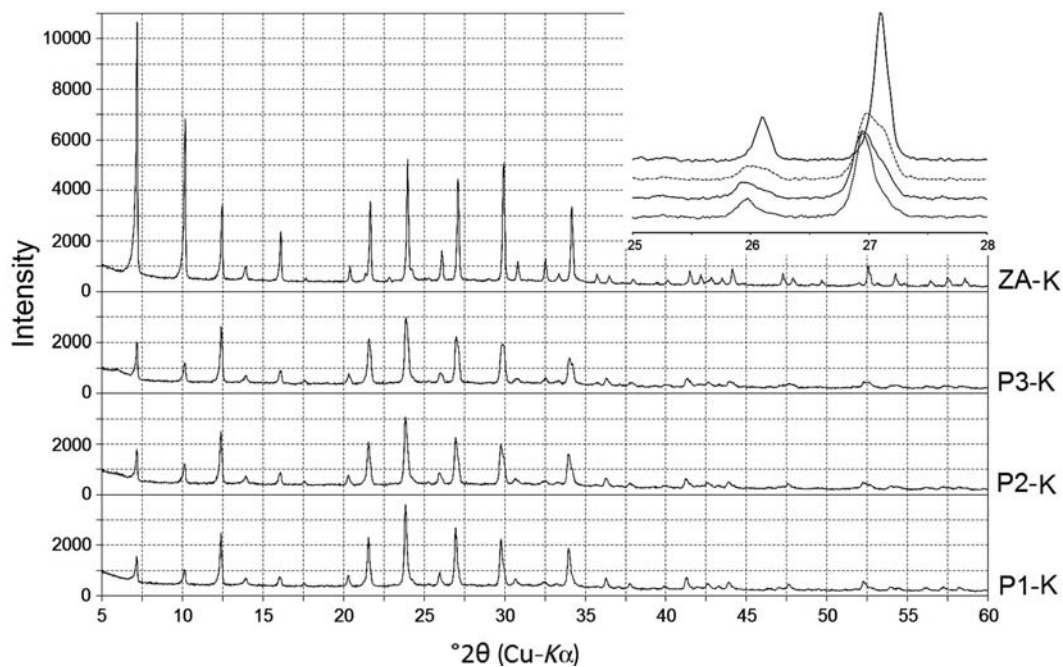


FIG. 8. XRD patterns of pigments obtained from Na-A zeolite derived from processed kaolin.

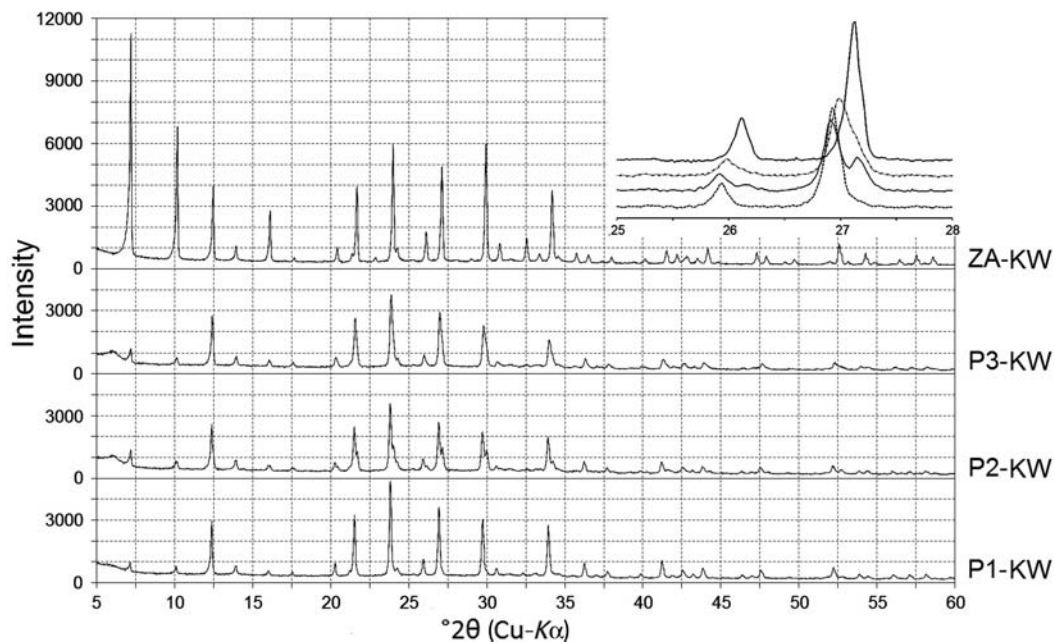


FIG. 9. XRD patterns of pigments obtained from Na-A zeolite derived from kaolin waste.

TABLE 4. Chemical compositions of the pigments.

Components (%)	ZA-K	ZA-KW	P1-K	P1-KW	P2-K	P2-KW	P3-K	P3-KW
SiO ₂	34.63	33.55	26.3	22.69	27.28	25.61	27.0	23.10
Al ₂ O ₃	29.57	28.13	22.66	19.58	22.96	21.96	23.11	19.88
SO ₃	–	–	19.22	23.71	14.93	18.41	15.03	22.07
Fe ₂ O ₃	0.34	0.3	0.28	0.19	0.23	0.234	0.23	0.205
TiO ₂	0.21	0.14	0.17	0.11	0.13	0.141	0.2	0.143
Na ₂ O	17.52	19.38	22.09	22.47	21.82	23.14	20.69	21.36
K ₂ O	<0.1	<0.1	<0.1	<0.1	<0.1	<0.1	<0.1	<0.1
CaO	<0.1	<0.1	<0.1	<0.1	<0.1	<0.1	<0.1	<0.1
P ₂ O ₅	<0.1	–	–	–	–	–	–	–
LOI	17.65	18.43	9.21	11.19	12.57	10.43	13.69	13.16

the finer particle size at 550°C and until total cooling. In addition, the precursor species S₅²⁻ must have dissociated preferentially into S₆²⁻ and S₄²⁻, which diffused rapidly to the zeolite interior and escaped from the successive dissociation stage that would lead to the blue chromophore S₃⁻ (Steufel, 2003). Thus, due to the lesser production of blue chromophores, the pigments derived from ZA-K presented lighter hues than those derived from ZA-KW.

Comparing the XRD patterns of the zeolites with those of their derived pigments, the LTA structure of the zeolite is observed to have been maintained (Figs 8 and 9). However, some changes take place related to the decrease in intensities and shifts of the peaks to the left of the 2θ axis, particularly in the region 25–28°2θ.

The effect of calcination on the XRD pattern of the zeolite was analysed using the sample that was calcined without sulfur or Na₂CO₃. All peak positions were maintained but showed a decrease in intensity of 12 to 18%, which is attributed to dehydration. Thus, the shifts in the 25–28°2θ region are clearly due to the insertion of chromophoric polysulfides in the zeolite pores and channels. This modification might be helpful in terms of understanding the structure of the zeolitic pigment.

Although the starting materials are apparently unique, the single peak at ~27°2θ becomes a double peak in the pigment, suggesting a mixture of the chromophores S₃⁻ and S₆²⁻ (Figs 8 and 9). The shape of this double peak in both series (-K and -KW) reinforces the structural and/or compositional differences between the pigments derived from zeolites with different particle sizes. This demonstrates once more the strong influence of this physical feature on the pigments' colours and hues.

The appearance of a new reflection at ~5.5°2θ in almost all pigments (and which is even more intense in the pigments derived from a coarser zeolite) must be related to the insertion of the chromophore S₃⁻, which is responsible for the blue colour. Finally, no change was observed in the sodalite peaks (Kowalak & Jankowska, 2003; Kowalak *et al.*, 2004; Loera *et al.*, 2006).

The formation and insertion of chromophores of sodium polysulfides in zeolite may be accompanied by an increase in sodium content and high sulfur levels in the chemical composition of the pigments (Table 4), which confirms the results discussed previously.

DISCUSSION

Previous studies from Raman spectroscopy have shown that polysulfides are obtained after consecutive reactions from homolytic dissociation, starting with sulfur fusion and subsequent sodium sulfide formation (Gobeltz *et al.*, 2011). The products of these reactions are related directly to the initial composition of the mixture and also to the temperature, as well as the particle size, which was confirmed during the present study.

According to Raman spectroscopy results it was possible to identify the bands responsible for the colours of the grains observed in the images, as noted in previous studies which used other instrumental techniques to detect the presence of the polysulfides (Teufel, 2003; Ledé *et al.*, 2007; Gobeltz *et al.*, 2011).

The formation of S₃⁻ in polysulfides occurs by homolytic dissociation of the S₆²⁻ and these chromophores migrate to the interior of the b- and a-cages of zeolite A (Gobeltz *et al.*, 2011). This may explain

the identification of S_3^- bands in the blue grains, S_6^{2-} bands in the yellow grains and both bands in the green grains. It also justifies XRD results that did not show changes in the crystal structure, but only peak displacement.

CONCLUSIONS

The use of kaolin waste in the production of zeolitic pigments is a promising option for the sustainable production of pigments. Indeed, ultramarine pigments were obtained with more interesting colour and hue variations than those obtained with processed kaolin. This effect on colour and hue was due mainly to the coarser particle size, which was shown to control the final appearance of the pigments.

Under the physicochemical conditions adopted, the blue colour and a dark green hue could only be obtained with the kaolin waste under the same reactant conditions as those used for the processed kaolin.

Raman analysis proved that the chromophore S_6^{2-} was responsible for the yellow colour and that S_3^- produces the blue colour. A mixture of the two resulted in the green colour that was predominant in the present work. A zeolite with a finer particle size favours the formation of S_6^{2-} whereas a zeolite with a coarser particle size favours the formation of S_3^- . In addition, the sulfur/ Na_2CO_3 ratio of 2:1 also favours the formation of S_3^- .

ACKNOWLEDGEMENTS

The authors are grateful to CNPq (Conselho Nacional de Desenvolvimento Científico e Tecnológico) for a scholarship to R.A. Menezes and research grant to R.S. Angélica (303.871/2010-5). Imerys Rio Capim Caulim SA is acknowledged gratefully for supplying kaolin samples (processed and waste) not only for the present study but also for other research projects in the authors' research group. Financial resources for this work were obtained from the following projects related to zeolite synthesis from Amazon kaolin: (1) Edital MCT/CT-Mineral/VALE/CNPq No 12/2009, 550.297/2010-3; and (2) Edital No 01/2010, FAPEMIG/FAPESP/FAPESPA/VALE, ICAAF No 027/2011.

REFERENCES

Alkan M., Hopa C., Yilmaz Z. & Guler H. (2005) The effect of alkali concentration and solid/liquid ratio on the hydrothermal synthesis of zeolite NaA from natural kaolinite. *Microporous and Mesoporous Materials*, **86**, 176–184.

- Barata M.S. & Angélica R.S. (2012) Caracterização dos resíduos caulínicos das indústrias de mineração de caulim da Amazônia como matéria-prima para produção de pozolanas de alta reatividade. *Cerâmica*, **58**, 36–42.
- Barata M.S., Angélica R.S., Pollmann H. & Costa M.L. (2005) The use of wastes derived from kaolin processing industries as a pozzolanic material for high-performance mortars and concrete. *European Journal of Mineralogy*, **17**, 10–10.
- Bieseki L., Penha F.G. & Pergher S.B.C. (2013) Zeolite A synthesis employing a Brazilian coal ash as the silicone and aluminum source and its application in adsorption and pigment formulation. *Materials Research*, **16**, 38–43.
- Booth D.G., Dann S.E. & Weller M. T. (2003) The effect of the cation composition on the synthesis and properties of ultramarine blue. *Dyes and Pigments*, **58**, 73–82.
- Brasil (2016) Ministério de Minas e Energia. Departamento Nacional de Produção Mineral. *Sumário Mineral*, Ministério de Minas e Energia, 135 pp. Brasília. Disponível em: <http://www.dnpm.gov.br>. Acesso em: 01/2016.
- Carneiro B.S., Angélica R.S., Scheller T., De Castro E.A. S. & Neves R.F. (2003) Caracterização mineralógica e geoquímica e estudo das transformações de fase do caulim duro da região do Rio Capim, Pará. *Cerâmica*, **49**, 273–244.
- Ding L., Yang H., Rahimi P., Omotoso O., Friesen W., Fairbridge C., Shi Y. & Ng S. (2010) Solid transformation of zeolite NaA to sodalite. *Microporous and Mesoporous Materials*, **130**, 303–308.
- Gerrits P.P.K., Vos D.E.D., Feijen E.J.P. & Jacobs P.A. (1997) Raman spectroscopy on zeolites. *Microporous Materials*, **8**, 3–17.
- Gobeltz N., Demortier A. & Lelieur J.P. (1998a) Identification of the products of the reaction between sulfur and sodium carbonate. *Inorganic Chemistry*, **37**, 136–138.
- Gobeltz N., Demotier A., Lelieur J.P. & Duhayon C. (1998b) Encapsulation of the chromophores into the sodalite structure during the synthesis of the blue ultramarine pigment. *Journal of the Chemical Society, Faraday Transactions*, **94**, 2257–2260.
- Gobeltz N., Ledé B., Raulin K., Demortier A. & Lelieur J. P. (2011) Synthesis of yellow and green pigments of zeolite LTA structure: Identification of their chromophores. *Microporous and Mesoporous*, **141**, 214–221.
- Heller-Kallai L. & Lapidés I. (2007) Reactions of kaolinites and metakaolinites with NaOH – comparison of different samples (part 1). *Applied Clay Science*, **35**, 99–107.
- Jankowska A. & Kowalak S. (2008) Synthesis of ultramarine analogs from erionite. *Microporous and Mesoporous Materials*, **110**, 570–578.
- Kowalak S. & Jankowska A. (2003) Application of zeolites as matrices for pigments. *Microporous and Mesoporous Material*, **61**, 213–222.

- Kowalak S., Pawłowska M., Miluška M., Stróżyk M., Kania J. & Przystajko W. (1995) Synthesis of ultramarine from synthetic molecular sieves. *Colloids and Surfaces*, **101**, 179–185.
- Kowalak S., Wróbel M., Gołębniak N., Jankowska A. & Turkot B. (1999) Zeolite matrices for pigments. *Studies in Surface Science and Catalysis*, **125**, 753–760.
- Kowalak S., Jankowska A. & Łączkowska S. (2004) Preparation of various color ultramarine from zeolite A under environment-friendly conditions. *Catalysis Today*, **90**, 167–172.
- Kowalak S., Jankowska A., & Łączkowska S. (2005) Influence of cations on color and structure of ultramarine prepared from zeolite A. *Studies in Surface Science and Catalysis*, **158**, 215–222.
- Lapides I. & Heller-Kallai L. (2007) Reactions of metakaolinite with NaOH and colloidal silica – comparison of different samples (part 2). *Applied Clay Science*, **35**, 94–98.
- Ledé B., Demortier A., Gobeltz N., Lelieur J.P., Picquenard E. & Duhayon C. (2007) Observation of the ν_3 Raman band of S_3^- inserted into sodalite cages. *Journal of Raman Spectroscopy*, **38**, 1461–1468.
- Lewicka E. (2016) Origin of colour after firing feldspar-quartz raw material from the Sobotka region (Lower Silesia, SW Poland). *Mineral Engineering Conference*, **8**, 01022.
- Loera S., Ibarra I.A., Laguna H., Lima E., Bosch P., Lara V. & Haro-Poniatowski E. (2006) Colored sodalite and A zeolites. *Industrial & Engineering Chemistry*, **45**, 9195–9200.
- Maia A.A.B., Saldanha E., Angélica R.S., Souza C.A.G. & Neves R.F. (2007) Utilização de rejeito de caulim da Amazônia na síntese da zeólita A. *Cerâmica*, **53**, 319–324.
- Maia A.A.B., Angélica R.S. & Neves R.F. (2008) Estabilidade térmica da zeólita A sintetizada a partir de um rejeito de caulim da Amazônia. *Cerâmica*, **54**, 345–350.
- Menezes R.A., Paz S.P.A., Angélica R.S., Neves R.F. & Pergher S.B.C. (2014) Color and shade parameters of ultramarine zeolitic pigments synthesized from kaolin waste. *Materials Research*, **17**, 23–27.
- Murad E. & Köster H.M. (1999) Determination of the Ti speciation in comercial kaolins by Raman spectroscopy. *Clay Minerals*, **34**, 479–485.
- Paz S.P.A., Angélica R.S. & Neves R.F. (2010) Síntese hidrotermal de sodalita básica a partir de um rejeito de caulim termicamente ativado. *Química Nova*, **33**, 579–583.
- Rigo R.T., Pergher S.B.C., Petkowicz D.I. & Santos J.H.Z. (2009) Um novo procedimento de síntese de zeólita A empregando argilas naturais. *Química Nova*, **32**, 21–25.
- Steufel R. (2003) *Elemental Sulfur and Sulfur Rich Compounds-II*. Springer, Berlin.
- Tarling S.E., Barnes P. & Klinowski J. (1988) The structure and Si, Al distribution of the ultramarines. *Acta Crystallographica*, **B44**, 128–135.